


## Proposal for a long-distance nonlocality test with entanglement swapping and displacement-based measurements

Anders J. E. Bjerrum,<sup>\*</sup> Jonatan B. Brask<sup>✉</sup>, Jonas S. Neergaard-Nielsen<sup>✉</sup>, and Ulrik L. Andersen<sup>✉</sup>  
*Center for Macroscopic Quantum States (bigQ), Department of Physics, Technical University of Denmark,  
 2800 Kongens Lyngby, Denmark*

 (Received 7 February 2023; revised 14 April 2023; accepted 3 May 2023; published 23 May 2023)

We analyze an all-optical setup which enables Bell-inequality violation over long distances by exploiting probabilistic entanglement swapping. The setup involves only two-mode squeezers, displacements, beamsplitters, and on-off detectors. We describe how events must be arranged to close both the detection and locality loopholes. We analyze a scenario with dichotomic inputs and outputs, and check the robustness of the Bell inequality violation for up to six parties, with respect to phase, amplitude, and dark count noise, as well as loss.

DOI: [10.1103/PhysRevA.107.052611](https://doi.org/10.1103/PhysRevA.107.052611)

### I. INTRODUCTION

As pointed out already by Boole in his work on probability theory, logical relations between observable events imply inequalities for the probabilities of their occurrence [1,2]. Bell later demonstrated that the inequalities implied by a local causal realist description of nature can be violated within quantum mechanics [3,4], implying that quantum mechanics cannot be recast as a local causal realist theory. Subsequent experimental investigations by Clauser, Aspect, and their collaborators [5–7] confirmed the nonlocal predictions of quantum mechanics, and nonlocality gradually became accepted as an aspect of nature. These early experiments were, however, not loophole-free, and while loophole-free violations have since been realized [8–11], it still remains experimentally challenging, with loss and detector inefficiencies being some of the main obstacles [12].

Loopholes constitute ways in which nature, or an eavesdropper, can arrange experimental outcomes, such that an experiment appears nonlocal, while in reality it is not. The detection loophole is relevant when inconclusive measurements are discarded from the experimental data [13]. Such inconclusive measurements typically occur due to losses during transmission of the particles or nonunit efficiency of the detectors. It has been demonstrated that discarding inconclusive measurement rounds renders it possible to violate a Bell inequality using classical optics [14]. The locality loophole is present if measurements are performed such that a subluminal signal can transfer information between measurement stations during a measurement sequence. Such a sequence includes the act of choosing a measurement basis and performing the measurement in this basis. The locality loophole can be closed by separating the measurement stations and keeping the duration of the measurement sequence short. However, this separation tends to induce losses and noise in the state shared by the participants of the experiment, and these losses

tend to make the shared quantum state local, i.e., it cannot be used to demonstrate a Bell inequality violation.

In spite of these difficulties, the utilization of nonlocality is now moving from fundamental science towards practical applications, where the provable nonlocality of a quantum state is used in device-independent protocols to certify the security of a cryptographic key [15–20]. Crucial to the realization of device-independent quantum key distribution is the ability to close relevant loopholes, and to demonstrate the violation of Bell inequalities across distances relevant for telecommunication.

In this work we propose an experiment capable of violating a Bell inequality when the parties are separated by channels of low transmission. Our experiment is designed to be capable of closing the detection and locality loopholes, and invokes only standard quantum optics tools, such as two-mode squeezers, displacements, and click detectors (on-off detectors). A sketch of the setup with  $N$  parties is shown in Fig. 1. The proposed experiment is inspired by the setup in [21], in which displacement-based measurements are used to demonstrate a Bell inequality violation. In our protocol, two-mode squeezers generate weakly squeezed two-mode squeezed vacuum states with half of each state sent a short distance to an on-off detector, and the other half sent to a distant interferometer B. The left-going modes in Fig. 1 are labeled  $p_n$ , and the right-going modes are labeled  $s_n$ ; we group them into two sets  $P = \{p_1, p_2, \dots, p_N\}$  and  $S = \{s_1, s_2, \dots, s_N\}$ . We use the same label for a mode and the corresponding detector. Each of the  $N$  detectors in  $P$  is considered as a party, with the possible measurement outcomes, click or no click, corresponding to whether any light arrives at the detector or not. The interferometer B mixes the modes  $S$ , so that a photon arriving at one of the input ports of B has an equal probability of triggering each of the detectors in  $S$ . We then require that only detector  $s_N$  clicks, and that the remaining detectors in  $S$  do not click. Hence our protocol is similar to an event-ready scheme [8,11,22] based on optical entanglement swapping [23–26], but without the need for quantum memories. Upon obtaining the correct measurement outcome at  $S$ , the measurement outcomes at the detectors in  $P$  are approximately

<sup>\*</sup>Corresponding author: [ajebje@dtu.dk](mailto:ajebje@dtu.dk)

the same as if the detectors measured the single-photon state  $\frac{1}{\sqrt{N}}(|1, 0, \dots, 0\rangle + |0, 1, \dots, 0\rangle + \dots + |0, 0, \dots, 1\rangle)$ , in the limit of vanishing squeezing. However, due to the presence of dark counts at the detectors it is not optimal to operate the experiment in the limit of vanishing squeezing, and the analyzed state will only be similar to a  $W$  state. The nonlocality of the  $W$  state was analyzed in [21,27–29], and we expect to see similar results for the state analyzed in this work. However, it is worth noting that the study in [28] focuses on single-run violations of locality, as opposed to the statistical violation analysed in this work. Moreover the measurements in [28] involved general qubit measurements, while we assume the more feasible displacement-based measurements.

Our work also differs in key aspects from the protocols in [21,27,29]. The purification step proposed in the present work is part of the state preparation, i.e., obtaining the correct measurement outcomes at  $S$  will mitigate loss incurred in the channels  $ch_s$  for suitable values of the squeezing parameters, while at the same time preparing a  $N$ -partite entangled state. In [27,29] the authors do not introduce a heralded step to mitigate loss, limiting the distance over which nonlocality can be demonstrated. In [21] loss is mitigated by each party filtering their part of the state using a quantum scissor [30]. However, quantum scissors require single-photon sources making the idea increasingly less practical as we increase the number of parties. Our purification step does not involve quantum scissors, hence no single-photon sources are required for our scheme.

Note that the state preparation in our scheme generates a  $N$ -partite entangled state *after* the  $N$  parties have measured on their parts of the shared state. This implies that the parties must discard obtained measurement outcomes if the subsequent heralding measurement at  $S$  fails, and this opens the door for the detection loophole. However, as we will show in the following, it turns out to be possible to arrange the events of the protocol such that the detection loophole is closed.

Prior to each detector in  $P$ , either of two different displacements (D in Fig. 1) is applied to the field. These displacements make up the two different measurement settings. We write the displacement applied on mode  $p \in P$  as  $X_p^{(n_p)} = (x_p^{(n_p)} \ y_p^{(n_p)})^T$ , with  $n_p \in (0, 1)$  labeling which of two possible displacements is implemented (measurement setting). We assume that all parties are choosing between the same two displacements when the phases of the  $N$  two-mode squeezers are the same. This assumption is invoked to simplify our analysis, and we found no advantage when deviating from it. The displacement operator for mode  $p$  is defined as

$$D_p(X_p^{(n_p)}) = \exp[i(\hat{q}_p y_p^{(n_p)} - \hat{p}_p x_p^{(n_p)})], \quad (1)$$

where  $\hat{q}_p$  and  $\hat{p}_p$  are the quadrature operators for mode  $p$ . We follow the convention  $[\hat{q}_k, \hat{p}_l] = 2i\delta_{kl}$ . From the quadrature operators we obtain the annihilation operator,  $\hat{a}_p = \frac{1}{2}(\hat{q}_p + i\hat{p}_p)$ . The coherent state generated by the displacement  $X_p^{(n_p)}$ , i.e., the state,  $|X_p^{(n_p)}\rangle = D_p(X_p^{(n_p)})|0\rangle$ , is centered on the coordinates  $(q_p \ p_p) = (2x_p^{(n_p)} \ 2y_p^{(n_p)})$  in phase space. We associate a click at a detector with the value 1, and no click

with the value  $-1$ . The observable associated with detector  $p$  is then given by

$$M_p = (I_p - |0\rangle_p\langle 0|) - |0\rangle_p\langle 0| \quad (2)$$

$$= I_p - 2|0\rangle_p\langle 0|, \quad (3)$$

where  $I_p$  is the identity operator associated with mode  $p$ . We may transfer the displacement applied prior to detector  $p$  onto the observable to obtain

$$M_p^{(n_p)} = I_p - 2| -X_p^{(n_p)} \rangle_p \langle -X_p^{(n_p)} |. \quad (4)$$

We attempt to violate the  $W^3ZB$  (Werner-Wolf-Weinfurter-Zukowski-Brukner) inequality [31–33],

$$2^{-N} \sum_b \left| \sum_n (-1)^{\langle b, n \rangle} \langle M^{(n)} \rangle \right| \leq 1. \quad (5)$$

$b$  and  $n$  are binary lists of length  $N$ , and the sums run over all possible binary lists.  $\langle b, n \rangle$  is the dot product between  $b$  and  $n$ . The entries of  $n$  label the measurement settings of the involved parties.  $\langle M^{(n)} \rangle$  is the correlator given by the product  $\langle M^{(n)} \rangle = \langle \prod_p M_p^{(n_p)} \rangle$ . We will refer to the left side of Eq. (5) as the Bell value of the  $W^3ZB$  inequality. The maximal violation of the  $W^3ZB$  inequality increases with the number of parties [34]. We therefore expect that when some loss and noise do not scale with the number of parties, then a violation of a  $W^3ZB$  inequality with more parties is more robust against this loss and noise, as compared to a  $W^3ZB$  inequality with fewer parties.

To close both the locality and detection loophole with two parties,  $p_1$  and  $p_2$ , we require that the events of the experiment are positioned as shown in the space-time diagram in Fig. 2. The events  $T_{p_1}$  and  $T_{p_2}$  correspond to the generation of two-mode squeezed vacuum for party  $p_1$  and party  $p_2$ , respectively. These events occur along a temporal (vertical) line, since the light emitted from the source has a finite duration  $\tau$ . For this reason there exists at each position  $x$  a duration of time where we expect the light to arrive with very high probability, this is marked with a darker shaded area. The measurements by  $p_1$  and  $p_2$  are labeled  $M_{p_1}$  and  $M_{p_2}$  respectively.  $M_s$  corresponds to the event where  $s_1$  and  $s_2$  measure. The choosing of measurement setting is labeled  $C_{p_1}$  and  $C_{p_2}$ . The measurements  $M_{p_1}$  and  $M_{p_2}$  collapse the temporal width of the pulses, as illustrated in the figure by an  $\times$ . The swap  $M_s$  occurs with very high probability along the vertical black line inside the central black and yellow dashed diamond. The backwards light cone for a swapping event will then typically be bounded by the dashed backwards light cone.

To close the detection loophole,  $p_1$  and  $p_2$  must choose their measurement settings at a time and place such that information about their choices cannot influence the swapping measurement  $M_s$  via a subluminal signal. If the experiment is executed in this way, then we anticipate that an eavesdropper cannot tamper with the swap to falsify nonlocal correlations [35]. Most swapping events will obey this requirement if  $C_{p_1}$  and  $C_{p_2}$  are outside the dotted backward time cone shown in Fig. 2. The critical distance  $d_c$ , which is the characteristic distance the event  $C_{p_2}$  must be separated from the two-mode squeezer  $T_{p_2}$ , can be found by geometric arguments as

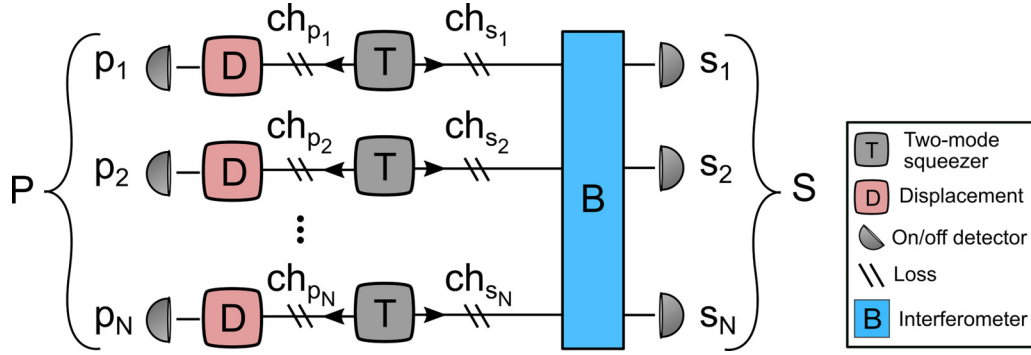


FIG. 1. Sketch of the analyzed setup with  $N$  parties. The left-going modes are labeled  $p_n$ , and the right-going modes are labeled  $s_n$ . A detector associated with a mode is given the same label as that mode. The measurement performed by the detectors in  $S$  effectively swaps the  $N$  bipartite entangled states, from the two-mode squeezers, into an  $N$ -mode entangled state. “ch” abbreviates channel.

$d_c = (1/2)c\tau$ , and is associated with a waiting time  $t_c = (1/2)\tau$ . Ideally  $p_2$  could make her choice of measurement setting at a distance  $d_c$  from  $T_{p_2}$ , at a time  $t_c$  after the light started to be emitted from the squeezer. Then her choice would most likely not be able to influence the swap  $M_s$ , while at the same time ensuring that the light pulse has not passed by her yet.

The experimental constraints discussed above generalize to the scenario where  $N$  parties attempt to obtain a Bell inequality violation, while closing the detection and locality loophole. That is, the parties should ensure that the events  $C_{p_n}$  are outside the backward timecone for the swapping event  $M_s$ . However, one should also ensure that the parties are sufficiently distant from each other, so that information on the choice of measurement setting and outcome cannot travel between parties during a measurement sequence.

## II. MODEL

We now give an outline of how we model the optical field, and how we include experimental imperfections in our analy-

sis. A full description can be found in Appendix A1. The fields generated by the two-mode squeezers are distributed in time and space according to some mode functions [36]. The amplitudes of these modes are quantum uncertain with Gaussian statistics described by a covariance matrix  $\sigma$  with elements  $\sigma_{kl} = 1/2(\langle\{Q_k, Q_l\}\rangle - \langle Q_k\rangle\langle Q_l\rangle)$ , where  $\{\cdot, \cdot\}$  denotes the anti-commutator and  $Q = Q_P \oplus Q_S$ , where  $Q_P = \bigoplus_{p \in P} (\hat{q}_p \ \hat{p}_p)$  with  $Q_S = \bigoplus_{s \in S} (\hat{q}_s \ \hat{p}_s)$  [37]. The corresponding density matrix, also describing the statistics of the field, is denoted  $\rho$ . We denote the squeezing parameter of the  $N$  squeezers as  $r$  and introduce the symbols,  $a = \sinh(2r)$  and  $v = \cosh(2r)$ . The covariance matrix of the  $2N$  modes can be written as

$$\sigma = \begin{pmatrix} v\mathbf{I} & \mathbf{R}_\phi \\ \mathbf{R}_\phi & v\mathbf{I} \end{pmatrix}, \quad (6)$$

where  $\mathbf{I}$  is the identity matrix of dimension  $2N$  and  $\mathbf{R}_\phi$  is the block diagonal matrix,

$$\mathbf{R}_\phi = \bigoplus_p \begin{pmatrix} a \cos(\phi_p) & -a \sin(\phi_p) \\ -a \sin(\phi_p) & -a \cos(\phi_p) \end{pmatrix}, \quad (7)$$

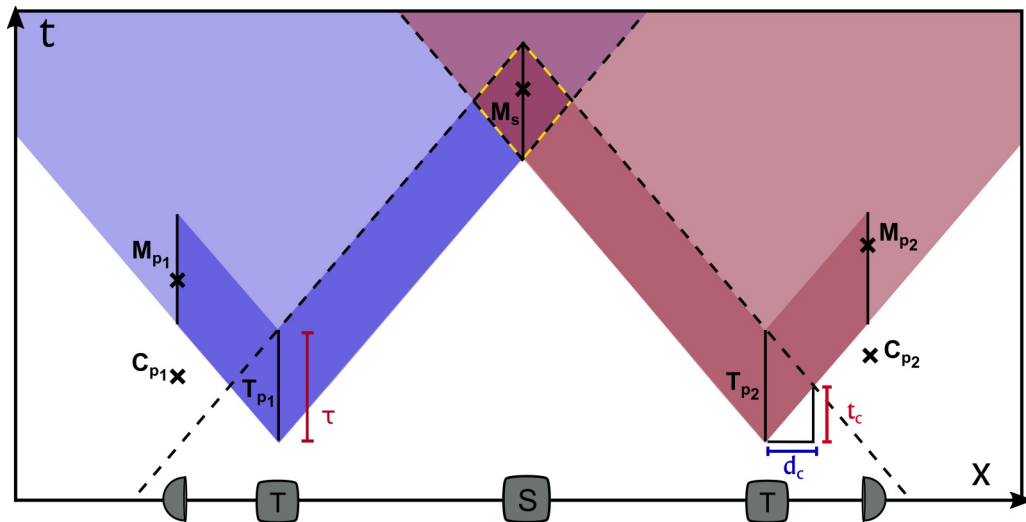


FIG. 2. Space-time diagram of a loophole-free experiment with two parties, showing the space-time ordering of important events (marked by  $\times$ ). The events  $T_{p_1}$  and  $T_{p_2}$  correspond to the generation of two-mode squeezed vacuum.  $C_{p_1}$  and  $C_{p_2}$  are the events where  $p_1$  and  $p_2$  decide their measurement settings.  $M_{p_1}$  and  $M_{p_2}$  correspond to events where  $p_1$  and  $p_2$  measure.  $M_s$  correspond to the event where  $s_1$  and  $s_2$  measure. At the bottom we sketch the experimental setup (compare with Fig. 1), where  $S$  corresponds to the swap following the interferometer  $B$ .

where  $\phi_p$  is the phase angle of the squeezer for party  $p$ . The expectation value of the field amplitude is assumed zero. The Wigner characteristic function corresponding to  $\rho$  is given by  $\chi_\rho(\Lambda) = \exp[-(1/2)\Lambda^T \Omega \sigma \Omega^T \Lambda]$  where  $\Lambda$  is a vector of conjugate quadratures (the Fourier transform dual to the quadratures) for the modes  $P$  and  $S$ , i.e.,  $\Lambda = \Lambda_P \oplus \Lambda_S$ , where  $\Lambda_P = \bigoplus_{p \in P} \Lambda_p$  and  $\Lambda_S = \bigoplus_{s \in S} \Lambda_s$ . The conjugate quadrature for mode  $k$  is a vector  $\Lambda_k = (\lambda_{kx} \quad \lambda_{ky})^T$ . We have also introduced the symplectic form  $\Omega = \bigoplus_{k=1}^{2N} \omega$ , where  $\omega$  is the antisymmetric matrix,

$$\omega = \begin{pmatrix} 0 & 1 \\ -1 & 0 \end{pmatrix}. \quad (8)$$

The modes  $S$  are then mixed on the interferometer B, and we assume that the corresponding mode functions are identical and have a high overlap at the beamsplitters making up the interferometer. Let  $\hat{a}_s$  be the amplitude operator for a mode  $s \in S$ , and the interferometer B is assumed to generate the Bogoliubov transformation,

$$\begin{pmatrix} \hat{a}_{s_1} \\ \hat{a}_{s_2} \\ \hat{a}_{s_3} \\ \vdots \\ \hat{a}_{s_N} \end{pmatrix} \rightarrow \frac{1}{\sqrt{N}} \begin{pmatrix} 1 & e^{i\frac{2\pi}{N}} & e^{i2\frac{2\pi}{N}} & \dots & e^{i(N-1)\frac{2\pi}{N}} \\ 1 & e^{i2\frac{2\pi}{N}} & e^{i4\frac{2\pi}{N}} & \dots & e^{i2(N-1)\frac{2\pi}{N}} \\ 1 & e^{i3\frac{2\pi}{N}} & e^{i6\frac{2\pi}{N}} & \dots & e^{i3(N-1)\frac{2\pi}{N}} \\ \vdots & \vdots & \vdots & \ddots & \vdots \\ 1 & 1 & 1 & \dots & 1 \end{pmatrix} \begin{pmatrix} \hat{a}_{s_1} \\ \hat{a}_{s_2} \\ \hat{a}_{s_3} \\ \vdots \\ \hat{a}_{s_N} \end{pmatrix}. \quad (9)$$

We condition the state on obtaining a click at detector  $s_N$  and no clicks at the remaining detectors, thereby heralding the conditional state  $\rho_c$  of modes  $P$ . The projector corresponding to this event is  $\hat{\Pi}_c = (\prod_{s \in \bar{S}} |0\rangle_s \langle 0|) (I_{s_N} - |0\rangle_{s_N} \langle 0|)$ , where  $\bar{S}$  is the set  $\bar{S} = S \setminus \{s_N\}$ . The conditional state is obtained as  $\rho_c = \text{Tr}_{\bar{S}}[\rho \hat{\Pi}_c] / P(C)$ , where  $P(C)$  is the normalization, i.e., the probability of obtaining the measurement outcomes heralding a successful swap.  $\hat{\Pi}_c$  has the characteristic function,

$$\begin{aligned} \chi_c(\Lambda_S) &= \text{Tr}[\hat{\Pi}_c D_S(\Lambda_S)] \\ &= E(\Lambda_{\bar{S}}) [\pi \delta^{(2)}(\Lambda_{s_N}) - E(\Lambda_{s_N})], \end{aligned} \quad (10)$$

where

$$E(\Lambda_j) = \exp\left(-\frac{1}{2} \Lambda_j^T \Lambda_j\right), \quad (11)$$

and  $\delta^{(2)}(\Lambda_j)$  is a delta function. We obtain the characteristic function of the conditional state through integration,

$$\chi_{\rho_c}(\Lambda_P) = \frac{1}{\pi^N P(C)} \int_{\mathbb{R}^{2N}} \chi_\rho(\Lambda) \chi_c(-\Lambda_S) d^{2N} \Lambda_S. \quad (12)$$

We then compute the Bell value of the W<sup>3</sup>ZB inequality by evaluating the expectation values  $\langle M^{(n)} \rangle = \langle \prod_{p \in P} M_p^{(n_p)} \rangle$ , for each setting  $n$ . This is done via the integral [38],

$$\begin{aligned} \left\langle \prod_{p \in P} M_p^{(n_p)} \right\rangle &= \text{Tr} \left\{ \rho_c \prod_{p \in P} M_p^{(n_p)} \right\} \\ &= \frac{1}{\pi^N} \int_{\mathbb{R}^{2N}} \chi_{\rho_c}(-\Lambda_P) \chi_M(\Lambda_P, X_P) d^{2N} \Lambda_P, \end{aligned} \quad (13)$$

where  $\chi_M(\Lambda_P, X_P)$  is the characteristic function associated with the observable  $\prod_{p \in P} M_p^{(n_p)}$ .  $X_P$  is a vector of the displacements applied prior to the detectors,  $X_P = \bigoplus_{p \in P} X_p^{(n_p)}$ . A closed form expression for  $\langle \prod_{p \in P} M_p^{(n_p)} \rangle$  can be found in Appendix A1.

### A. Noise model

We now outline how we describe noise relevant to the experiment. We will include dark counts in the detectors, loss in the channels, phase noise in the channels and measurements, and, finally, amplitude noise in the measurements. Amplitude and phase noise during measurement are expected to arise if imperfect displacements are applied.

We include dark counts in our measurement model by adding a noise term to the observable. Given that  $p_d$  is the probability of getting a dark count at a given detector, then we measure the observable,

$$\begin{aligned} M_p^{(n_p)} &= (1 - p_d) [I_p - 2|-X_p^{(n_p)}\rangle_p \langle -X_p^{(n_p)}|] + p_d I_p \\ &= I_p - 2(1 - p_d) |-X_p^{(n_p)}\rangle_p \langle -X_p^{(n_p)}|. \end{aligned} \quad (14)$$

If a given detector in  $S$  is triggered by a dark count with probability  $p_d$ , then the swap results in the transformation (see Appendix A1)

$$\rho \rightarrow \rho_c = \frac{1}{P(C)} \text{Tr}_S[\rho \tilde{\Pi}_c]. \quad (15)$$

We have introduced the operator  $\tilde{\Pi}_c$ ,

$$\tilde{\Pi}_c = (1 - p_d)^{N-1} \left( \prod_{s \in \bar{S}} |0\rangle_s \langle 0| \right) (I_{s_N} - (1 - p_d) |0\rangle_{s_N} \langle 0|). \quad (16)$$

We now describe how channel loss and detector efficiency are included in our model. Given that channel  $\text{ch}_{p_n}$  has transmission  $\eta_{p_n}$  and channel  $\text{ch}_{s_k}$  has transmission  $\eta_{s_k}$ , we model loss by a Gaussian map acting on the covariance matrix  $\sigma$  as [38],

$$\sigma \rightarrow G_\eta^{1/2} \sigma G_\eta^{1/2} + (I - G_\eta), \quad (17)$$

with the diagonal matrix  $G_\eta = G_{\eta_P} \oplus G_{\eta_S}$ , where  $G_{\eta_P} = \text{Diag}[\bigoplus_{p \in P} (\eta_p \quad \eta_p)]$  and  $G_{\eta_S} = \text{Diag}[\bigoplus_{s \in S} (\eta_s \quad \eta_s)]$ . We will assume that  $\eta_{p_n}$  equals  $\eta_P$ , i.e., the channels  $\text{ch}_P = \{\text{ch}_{p_1}, \text{ch}_{p_2}, \dots, \text{ch}_{p_N}\}$  have the same transmission. Likewise we assume that  $\eta_{s_k}$  equals  $\eta_S$ .  $\eta_d$  is the efficiency of a detector, and  $1 - \eta_d$  is the loss of the detector. Given that  $\eta_d$  is the same for all detectors in  $S$ , detector loss can then be commuted through B and absorbed into the transmission of the channels  $\text{ch}_S = \{\text{ch}_{s_1}, \text{ch}_{s_2}, \dots, \text{ch}_{s_N}\}$ . Likewise, the detector loss in  $P$  can be shifted to be prior to the displacements, if we attenuate the magnitude of the displacements by the factor  $\sqrt{\eta_d}$ .

We now turn to the problem of how to model phase noise. A phase perturbation of the state  $\rho$ , e.g., caused by environmental disturbance, can be modeled as a stochastic rotation in phase space,

$$\rho = \int d^N \theta P(\theta) R(\theta) \rho_0 R(-\theta), \quad (18)$$



TABLE I. Standard settings for noise parameters.  $\eta_P$  is the transmission of the channels  $ch_P$  ( $ch_{p_1}, ch_{p_2}, \dots$ ).  $\eta_S$  is the transmission of channels  $ch_S$ .  $\sigma_A$  is the standard deviation of the relative amplitude distribution ( $\sigma_A^2 = V_A$ ).  $\sigma_\theta$  is the standard deviation of the phase angle distribution ( $\sigma_\theta^2 = V_\theta$ ).  $p_d$  is the probability of getting a dark count at a given detector (e.g.,  $p_n$  or  $s_n$ ) during the measurement interval (which is assumed to be  $\tau$  in our analysis).

$\eta_P$	$\eta_S$	$\sigma_A$	$\sigma_\theta$	$p_d$
0.9	0.2	3/100	100 mrad	1/10 000

where  $\rho_0$  is the unperturbed state, and  $\theta$  is a vector of stochastic rotation angles  $\theta_p$  for  $p \in P$ , each being a perturbation on the phase of the corresponding mode. Note that phase noise acting on channels  $ch_S$  is shifted to act on channels  $ch_P$  instead.  $R(\theta)$  is the rotation operator  $R(\theta) = \prod_{p \in P} R_p(\theta_p)$ .  $R_{p_n}(\theta_{p_n})$  is applied just prior to the displacement operation on mode  $p_n$  and includes phase noise resulting from propagation in the channels  $ch_{p_n}$  and  $ch_{s_n}$ , and also the phase noise in the subsequent displacement operation. We make the assumption that the angles  $\theta$  are uncorrelated and model the probability density  $P(\theta)$  as a product of normal distributions for each angle  $\theta_p$ . The variance of  $\theta_p$  is labeled as  $V_\theta$ , and is the same for all modes. The correlated phase noise resulting from the interferometer B cannot be entirely captured by this simple model, but we expect that our model is sufficiently close to reality to indicate the sensitivity of the experiment toward phase noise. We furthermore assume that the angles  $\theta_p$  are small, allowing us to approximate the rotation of a coherent state by a small linear translation in phase space.

Finally, we describe how we model amplitude noise. Amplitude noise arises from an imperfect displacement and is modeled similarly to phase noise, with the rotation operator in Eq. (18) replaced by a displacement operator. The stochastic displacement on mode  $p$  is given relative to the displacement  $X_p^{(n_p)}$  applied on mode  $p$ , i.e., for mode  $p$  we obtain the stochastic displacement  $\epsilon_p X_p^{(n_p)}$ , where  $\epsilon_p$  is referred to as the relative amplitude. We assume that the relative amplitudes  $\epsilon_p$  are normal, independent, and identically distributed, with variance  $V_A$ . A more detailed description of the noise model can be found in Appendix A1.

### III. RESULTS AND DISCUSSION

We compute Bell values under varying experimental conditions. In order to obtain realistic values we must include in the model reasonable experimental errors. We choose the noise parameters shown in Table I. Unless otherwise stated, these are the values used for the noise parameters throughout our analysis. For instance, if we vary  $\eta_P$ , as is done in Fig. 6, then the remaining noise parameters are set at the values listed in Table I.

We maximize the violation of the  $W^3ZB$  inequality in the squeezing parameter  $r$ . The Bell value as a function of  $r$ , for the optimal choice of measurement settings, is shown in Fig. 3. We clearly observe that there exists an optimal squeezing value for which the Bell value is maximized, and that the optimal squeezing depends on the number of parties.

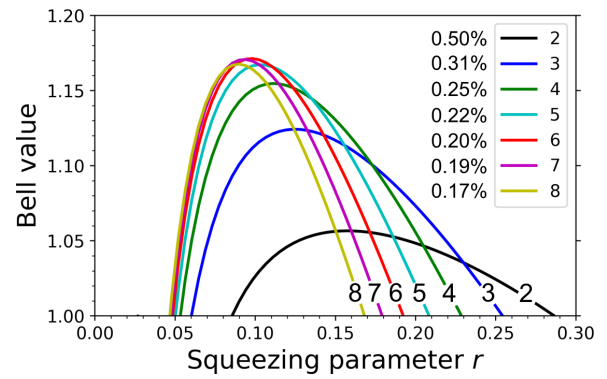


FIG. 3. Bell value of the  $W^3ZB$  inequality against the squeezing parameter  $r$  for different number of parties. The annotation and legend give the number of parties. The Bell value is computed for the optimal measurement settings at the given value of  $r$ . We observe a maximum in the Bell value at a particular squeezing. Next to the legend we list the probability  $P(C)$  that an experiment succeeds with that number of parties, at the corresponding optimal value of  $r$  (the value of  $r$  giving the largest Bell value).

We also observe that the maximal Bell value increases for more parties, until six parties, at which point the maximal Bell value decreases for more parties. While the correlations between all parties lead to a violation of the  $W^3ZB$  inequality at the optimal squeezing, we find that, for up to four parties, the marginal outcome probabilities describing any subgroup of parties are inside the Bell polytope, with the used measurement settings. This was evidenced by a linear program (see Appendix A2) and indicates that in these cases nonlocality results from correlations between *all* parties. An exception can occur for five parties if  $\eta_P$  is above 97%, and for six parties if  $\eta_P$  is above 91%, with the used measurement settings. In these cases a Bell inequality can be broken with a subgroup of four and five parties, respectively.

We find the optimal displacements (measurement settings) at the optimal squeezing for which the violation is maximized. The optimal displacement for party  $p_1$  and another party  $p_n$  are shown in Fig. 4. The phase angles of the two-mode squeezers belonging to  $p_1$  and  $p_n$  respectively, are labeled as  $\phi_{p_1}$  and  $\phi_{p_n}$ .  $m_0^{(p_1)}$  and  $m_1^{(p_1)}$  are the displacements used by party  $p_1$ , whereas  $m_0^{(p_n)}$  and  $m_1^{(p_n)}$  are the displacements used by party  $p_n$ .  $m_0^{(p_1)}$  and  $m_0^{(p_n)}$  have the same magnitude, but the displacements are directed along different quadrature axes at an angle  $\phi_{p_1} - \phi_{p_n}$ , and likewise for  $m_1^{(p_1)}$  and  $m_1^{(p_n)}$ . So the displacements used by a given party  $p_n$  will be determined

TABLE II. Magnitudes of the optimal displacements shown in Fig. 4 for the optimal value of  $r$ . If the detector transmission is  $\eta_d$ , then the magnitudes should be multiplied by  $1/\sqrt{\eta_d}$ .

No. of parties	$m_0$	$m_1$
2	0.59	-0.18
3	0.47	-0.20
4	0.41	-0.19
5	0.37	-0.18
6	0.33	-0.17

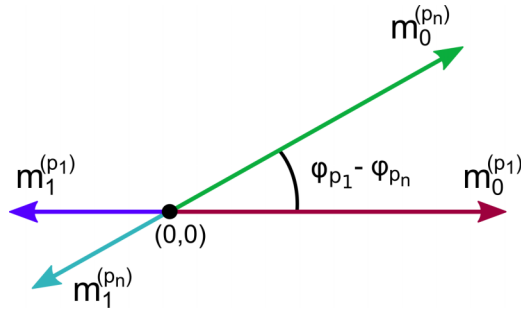


FIG. 4. The orientation of the optimal displacements (measurement settings) that the parties  $p_1$  and  $p_n$  should use to obtain a maximal violation of the  $W^3ZB$  inequality.  $m_0^{(p_1)}$  and  $m_1^{(p_1)}$  are the displacements used by party  $p_1$ , whereas  $m_0^{(p_n)}$  and  $m_1^{(p_n)}$  are the displacements used by party  $p_n$  (any party).  $p_n$ 's displacements should be at the angle  $\phi_{p_1} - \phi_{p_n}$  relative to  $p_1$ 's displacements, where  $\phi_{p_1}$  and  $\phi_{p_n}$  are the phase angles of the two-mode squeezers belonging to  $p_1$  and  $p_n$ . The magnitudes of  $m_0^{(p_n)}$  and  $m_1^{(p_n)}$  depend on the number of parties and are listed in Table II.

by the phase angle of their squeezer  $\phi_{p_n}$ . The magnitudes of  $m_0^{(p_n)}$  and  $m_1^{(p_n)}$  depend on the number of parties and are listed in Table II. The overall orientation of the quadrature axes is arbitrary, i.e., we can freely rotate Fig. 4, as long as the angle between displacements remain unchanged. In this sense, the displacements used by party  $p_1$  serve as a reference from which we can define the displacements to be used by the remaining parties.

We note that the optimum in squeezing, seen in Fig. 3, is the result of a competition between the dark count rate and the multiphoton generation rate. A dark count would render the measurements by the parties uncorrelated, thereby lowering the Bell value. This indicates that it is preferable to have high squeezing, so that photons from the optical field outnumber the dark counts. However, the click detectors in  $S$  cannot distinguish between one or more photons. Multiphoton emission from the two-mode squeezers therefore creates mixedness in the conditional state generated by the swap, and

this mixedness weakens the correlations between the measurement outcomes obtained by the parties. This mixedness can be avoided by lowering the degree of squeezing, so that on average less than one photon reaches the detectors in  $S$ . As a result, there is some amount of squeezing where the combined detrimental effect of dark counts and multiphoton generation is minimized. As we increase the number of parties, the presence of dark counts becomes more detrimental due to the increased number of detectors and the lower probability of a successful swap  $P(C)$ . This is the cause of the decrease in maximal Bell value for seven and eight parties, as compared to the case with six parties.

We investigate the sensitivity of the experiment toward the probability of a dark count at a given detector in  $S$ , and the result can be seen in Fig. 5 (left) for different number of parties. The probability of a dark count at a given detector in  $P$  is fixed at 0.01%. A dark count at detector  $s_N$  would mistakenly herald nonlocal correlations between the detectors in  $P$ , when no such correlations actually exists. This erroneous heralding significantly lowers the calculated Bell value. The Bell value is found to rapidly decrease around 0.02%. At this point, the probability of getting a dark count is no longer insignificant compared with the probability of generating the conditional state, which is in the range 0.2% to 0.5%, depending on the number of parties (see Fig. 3). For the case of two parties, the decrease in Bell value proceeds a bit slower; however, the lower initial Bell value (1.09) results in the curve reaching the classical limit of 1 at smaller dark count probabilities. The drop in Bell value for increasing probability of a dark count is in part due to the squeezing no longer being optimal. However, our calculations indicate that if  $p_d$  exceeds 0.05%, then the experiment cannot be used to violate the  $W^3ZB$  inequality, given the remaining errors (Table I), even at the corresponding optimal squeezing and measurement settings, and for any number of parties.

We also analyze the robustness of the Bell inequality violation against the probability of a dark count at a given detector in  $P$ , while the probability of a dark count at a given detector in  $S$  is fixed at 0.01%. A plot of this is shown in Fig. 5 (right)

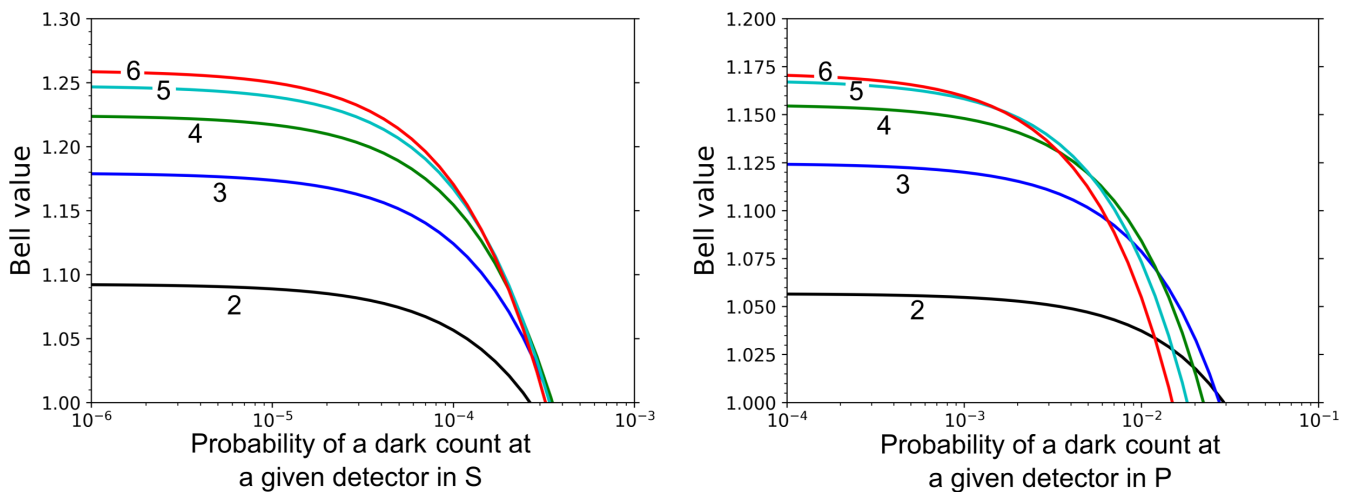


FIG. 5. Left: Bell value of the  $W^3ZB$  inequality against the probability of a dark count at a given detector in  $S$  during the measurement interval. The annotation indicates the number of parties. Right: Bell value of the  $W^3ZB$  inequality against the probability of a dark count at a given detector in  $P$  during the measurement interval.

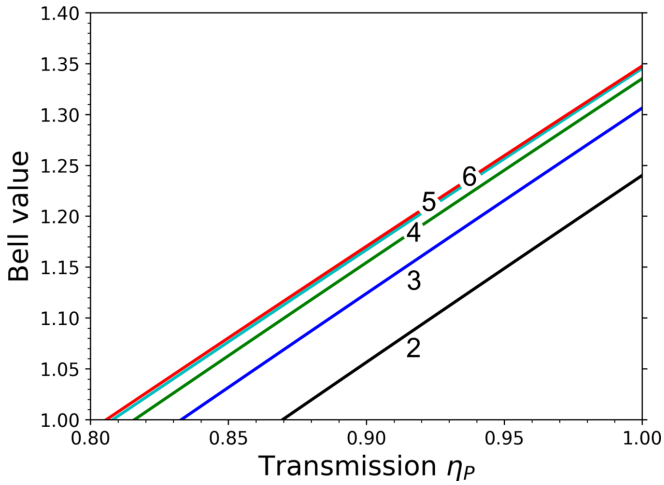


FIG. 6. Plot of how the Bell value of the  $W^3ZB$  inequality depends on the transmission of the channels  $ch_P$ , connecting the two-mode squeezers to the detectors in  $P$ . The annotation indicates the number of parties.

and clearly illustrates that the violation is highly robust against this probability.

The impact of loss on the Bell value of the  $W^3ZB$  inequality is shown in Figs. 6 and 7. In Fig. 6 we vary the transmission  $\eta_P$  and show how the Bell value changes. The transmission at which the Bell value drop below one lowers as we increase the number of parties. This indicates that a demonstration of nonlocality might be easier to realize when using more parties. In Fig. 7 we show the dependence of the Bell value on the transmission  $\eta_S$ . We observe that the Bell value is only weakly dependent on this transmission until a critical point around a transmission of 10%. The probability  $P(C)$  of successfully generating the conditional state, heralded by detector  $s_N$  click-

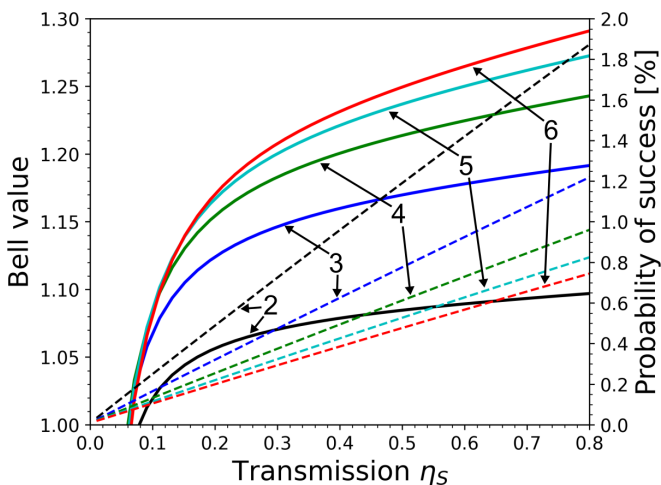


FIG. 7. Plot of how the Bell value of the  $W^3ZB$  inequality depends on the transmission of the channels  $ch_S$ , connecting the two-mode squeezers to the swapping detectors  $S$ . The annotation indicates the number of parties. The solid curves correspond to Bell values and match the left y axis. The dashed curves are the corresponding probabilities of generating the conditional state  $P(C)$ ; these drop as we lower the transmission  $\eta_S$ .

ing and the remaining detectors in  $S$  staying silent, is seen to drop linearly for decreasing transmission. If we assume a fiber loss of 0.3 dB/km, we find that a transmission of 10% corresponds to approximately 30 km. The maximal achievable separation between two parties will then be around 60 km.

We then check the sensitivity of the experiment against phase and amplitude noise. The result is shown in Fig. 8. In Fig. 8 (left) we plot the Bell value against the standard deviation of the relative amplitude distribution,  $\sigma_A$ . In Fig. 8 (right) we plot the Bell value against the standard deviation of the phase distribution,  $\sigma_\theta$ . We observe that the Bell value is not very sensitive to amplitude and phase noise. This implies that the optimal displacements, shown in Table II and Fig. 4, are not so strict, and that slight deviations from these displacements are acceptable.

#### IV. CONCLUSION

We have proposed an experiment for demonstrating nonlocality with multiple parties separated by a set of lossy channels. The experiment utilizes only standard quantum optical elements, including on-off detectors, beamsplitters, two-mode squeezers, and displacements. We have given a detailed account of how loss impacts the experiment, and identified critical values for channel transmissions, required for a Bell inequality violation with dichotomic inputs and outputs. We found that the experiment is very robust against loss in the channels connecting the parties ( $ch_S$ ), allowing for transmissions as low as 10%. On the other hand, our calculations indicate that the nonlocality of the experiment is strongly impacted by loss in the channels connecting the two-mode squeezer of each party to the detector associated with that party (channels  $ch_P$ ). However, we found that the experiment could be made more robust against loss in channels  $ch_P$  if the number of parties is increased. With four parties we found that the  $W^3ZB$  inequality could be violated for transmissions of channels  $ch_P$  as low as 82%. For an experiment with four or fewer parties, we found that the marginal outcome probabilities for all possible subgroups were inside the Bell polytope, with the used measurement settings.

Due to the heralded nature of the experiment, it is very sensitive toward dark counts at the heralding detector. Our calculations indicate that the probability of a dark count at a given detector during a measurement must not be much higher than 1 in 10 000, or the experiment fails. We then examined the influence of amplitude and phase noise, and found that the experiment is quite robust against these noise sources. The phase noise could be as high as several hundred milliradians, and the relative amplitude noise could be in excess of 25%.

#### ACKNOWLEDGMENTS

This work was supported by the European Union's Horizon Europe research and innovation programs under the project "Quantum Security Networks Partnership" (QSNP, Grant Agreement No. 101114043) and the Danish National Research Foundation, Center for Macroscopic Quantum States (bigQ, D NRF142) and a research grant (40864) from VIL-LUM FONDEN.

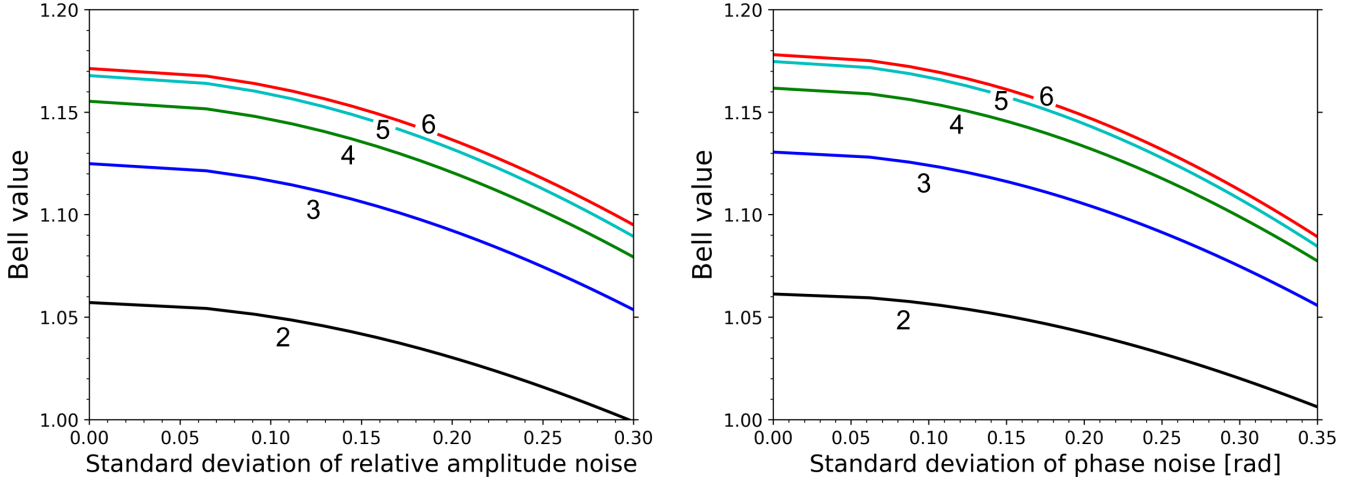


FIG. 8. Left: Plot of how the Bell value of the  $W^3ZB$  inequality depends on amplitude noise ( $\sigma_A$ ). The annotation indicates the number of parties. Right: Plot of how the Bell value depends on the phase noise ( $\sigma_\theta$ ).

APPENDIX

1. A1

The state  $\rho$  is generated by  $N$  two-mode squeezers and occupies the modes  $S$  and  $P$ . The characteristic function of  $\rho$  is given by  $\chi_\rho(\Lambda) = \exp[-(1/2)\Lambda^T \Omega \sigma \Omega^T \Lambda]$  where  $\Lambda$  is a vector of conjugate quadratures for the modes in  $S$  and  $P$ . We introduce the following decomposition of the covariance matrix of  $\rho$ :

$$\sigma = \begin{pmatrix} \sigma_P & K_{\bar{S}} & K_{s_N} \\ K_{\bar{S}}^T & \sigma_{\bar{S}} & C \\ K_{s_N}^T & C^T & \sigma_{s_N} \end{pmatrix}. \tag{A1}$$

We also introduce the matrices

$$K_{\bar{S}} = (K_{\bar{S}} \ K_{s_N}), \quad \sigma_{\bar{S}} = \begin{pmatrix} \sigma_{\bar{S}} & C \\ C^T & \sigma_{s_N} \end{pmatrix}. \tag{A2}$$

The subscript refers to the modes described by the relevant submatrix, i.e.,  $\sigma_{\bar{S}}$  describes the marginal distribution of the modes  $\bar{S} = S \setminus \{s_N\}$ .

The modes in  $S$  are mixed in the interferometer B, described by the Bogoliubov transformation in Eq. (9). We then condition the state on obtaining a click at detector  $s_N$  and no click at the remaining detectors in  $S$  (this is referred to as a swap). If the detectors in  $S$  are triggered by a dark count with probability  $p_d$ , then the swap might herald success under three different conditions,

(1) No dark counts occur. Light reaches detector  $s_N$  and no light reaches the remaining detectors in  $S$ . This event is associated with the projector  $\hat{\Pi}_1 = (\prod_{s \in \bar{S}} |0\rangle_s \langle 0|) (I_{s_N} - |0\rangle_{s_N} \langle 0|)$ .

(2) A dark count occurs at detector  $s_N$ . Light reaches detector  $s_N$ , and no light reaches the remaining detectors in  $S$ . This event is associated with the projector  $\hat{\Pi}_1 = (\prod_{s \in \bar{S}} |0\rangle_s \langle 0|) (I_{s_N} - |0\rangle_{s_N} \langle 0|)$ .

(3) A dark count occurs at detector  $s_N$ . No light reaches any detectors in  $S$ . This event is associated with the projector  $\hat{\Pi}_2 = \prod_{s \in S} |0\rangle_s \langle 0|$ .

Let  $P(\hat{\Pi}_n|C)$  be understood as the probability that the event  $\hat{\Pi}_n$  occurs, given that detectors  $S$  herald a successful swap

$C$ .  $P(\hat{\Pi}_n) = \text{Tr}[\hat{\Pi}_n \rho]$  is the prior probability that the event  $\hat{\Pi}_n$  occurs. The swap then transform the state  $\rho$  into the conditional state  $\rho_c$  as

$$\begin{aligned} \rho &\rightarrow \rho_c \\ &= \text{Tr}_S \left[ P(\hat{\Pi}_1|C) \frac{\hat{\Pi}_1 \rho \hat{\Pi}_1}{P(\hat{\Pi}_1)} + P(\hat{\Pi}_2|C) \frac{\hat{\Pi}_2 \rho \hat{\Pi}_2}{P(\hat{\Pi}_2)} \right] \\ &= \text{Tr}_S \left[ \rho \left( P(\hat{\Pi}_1|C) \frac{\hat{\Pi}_1}{P(\hat{\Pi}_1)} + P(\hat{\Pi}_2|C) \frac{\hat{\Pi}_2}{P(\hat{\Pi}_2)} \right) \right]. \end{aligned} \tag{A3}$$

By Bayes' theorem we have

$$\frac{P(\hat{\Pi}_n|C)}{P(\hat{\Pi}_n)} = \frac{P(C|\hat{\Pi}_n)}{P(C)}, \tag{A4}$$

which gives another expression for  $\rho_c$ ,

$$\begin{aligned} \rho_c &= \text{Tr}_S \left[ \rho \left( \frac{P(C|\hat{\Pi}_1)}{P(C)} \hat{\Pi}_1 + \frac{P(C|\hat{\Pi}_2)}{P(C)} \hat{\Pi}_2 \right) \right] \\ &= \frac{1}{P(C)} \text{Tr}_S[\rho \tilde{\Pi}_c], \end{aligned} \tag{A5}$$

where we have introduced the operator  $\tilde{\Pi}_c$ ,

$$\tilde{\Pi}_c = P(C|\hat{\Pi}_1) \hat{\Pi}_1 + P(C|\hat{\Pi}_2) \hat{\Pi}_2. \tag{A6}$$

The probability of the swap being heralded as successful, given that the event  $\hat{\Pi}_1$  occurs, is given by  $P(C|\hat{\Pi}_1) = (1 - p_d)^N + (1 - p_d)^{N-1} p_d$ , i.e., the swap will succeed as long as no dark count triggers any detector other than  $s_N$ . If no light reaches any detectors in  $S$ , then the swap can be heralded as successful only if a dark count triggers detector  $s_N$ , so  $P(C|\hat{\Pi}_2) = (1 - p_d)^{N-1} p_d$ . Then we have

$$\begin{aligned} \tilde{\Pi}_c &= (1 - p_d)^N \hat{\Pi}_1 + (1 - p_d)^{N-1} p_d (\hat{\Pi}_1 + \hat{\Pi}_2) \\ &= (1 - p_d)^{N-1} \left( \prod_{s \in \bar{S}} |0\rangle_s \langle 0| \right) [I_{s_N} - (1 - p_d) |0\rangle_{s_N} \langle 0|]. \end{aligned} \tag{A7}$$



A different number of photons could *in principle* be distinguishable by the detector, even if the experimenter cannot distinguish the detector states sufficiently well to obtain this information. We define a projector onto Fock states,  $\hat{\Pi}^{(n)} = (\prod_{s \in \bar{S}} |0\rangle_s \langle 0|) |n\rangle_{s_N} \langle n|$ . If different Fock states are in principle distinguishable, then the transformation of  $\rho$ , conditioned on the swap, ought to be

$$\begin{aligned} \rho &\rightarrow \text{Tr}_S \left[ \sum_{n=0}^{\infty} P(\hat{\Pi}^{(n)}|C) \frac{\hat{\Pi}^{(n)} \rho \hat{\Pi}^{(n)}}{P(\hat{\Pi}^{(n)})} \right] \\ &= \text{Tr}_S \left[ \rho \sum_{n=0}^{\infty} \frac{P(\hat{\Pi}^{(n)}|C)}{P(\hat{\Pi}^{(n)})} \hat{\Pi}^{(n)} \right]. \end{aligned} \quad (\text{A8})$$

Using Bayes' theorem we have

$$\begin{aligned} &= \frac{1}{P(C)} \text{Tr}_S \left[ \rho \sum_{n=0}^{\infty} P(C|\hat{\Pi}^{(n)}) \hat{\Pi}^{(n)} \right] \\ &= \frac{1}{P(C)} \text{Tr}_S [\rho \tilde{\Pi}'_c]. \end{aligned} \quad (\text{A9})$$

We then make the assumption that

$$P(C|\hat{\Pi}^{(n)}) = \begin{cases} (1-p_d)^N + (1-p_d)^{N-1} p_d, & \text{if } n > 0 \\ (1-p_d)^{N-1} p_d, & \text{if } n = 0. \end{cases} \quad (\text{A10})$$

Under this assumption one can show that  $\tilde{\Pi}'_c = \tilde{\Pi}_c$ , and it doesn't matter whether we use the transformation in Eq. (A3) or in Eq. (A8).

The characteristic function of  $\tilde{\Pi}_c$  is given by

$$\begin{aligned} \chi_c(\Lambda_S) &= \text{Tr}_S [\tilde{\Pi}_c D_S(\Lambda_S)] = (1-p_d)^{N-1} E(\Lambda_{\bar{S}}) [\pi \delta^{(2)}(\Lambda_{s_N}) \\ &\quad - (1-p_d) E(\Lambda_{s_N})]. \end{aligned} \quad (\text{A11})$$

Then we have that

$$\begin{aligned} \rho_c &= \frac{1}{P(C)} \text{Tr}_S [\rho \tilde{\Pi}_c] = \frac{1}{P(C)} \int_{\mathbb{R}^{4N}} D_P(-\Lambda_P) \\ &\quad \chi_\rho(\Lambda_P, \Lambda_S) \chi_c(-\Lambda_S) \frac{d^{4N} \Lambda}{\pi^{2N}}. \end{aligned} \quad (\text{A12})$$

In evaluating the above expression we have used Glauber's formula [38] to express  $\rho$  and  $\tilde{\Pi}_c$  in terms of their characteristic functions ( $\chi_\rho$  and  $\chi_c$ ),

$$\hat{O} = \int_{\mathbb{R}^{2n}} \frac{d^{2n} B}{\pi^n} \chi_O(B) D^\dagger(B), \quad (\text{A13})$$

where  $n$  is the number of modes. We also used the facts

$$\text{Tr}_i [D(\Lambda_i)] = \pi \delta^{(2)}(\Lambda_i), \quad (\text{A14})$$

$$D(\Lambda_i) D(\Lambda_j) = D(\Lambda_i + \Lambda_j) \exp[-i \Lambda_i^T \omega \Lambda_j]. \quad (\text{A15})$$

From Eq. (A12) we may read off the characteristic function of the conditional state  $\rho_c$ ,

$$\chi_{\rho_c}(\Lambda_P) = \frac{1}{\pi^N P(C)} \int_{\mathbb{R}^{2N}} \chi_\rho(\Lambda_P, \Lambda_S) \chi_c(-\Lambda_S) d^{2N} \Lambda_S. \quad (\text{A16})$$

Inserting the expressions for  $\chi_\rho$  and  $\chi_c$ , we may evaluate the conditional state as

$$\chi_{\rho_c}(\Lambda_P) = \frac{(1-p_d)^{N-1}}{P(C)} [\chi_{\bar{S}}(\Lambda_P) - (1-p_d) \chi_S(\Lambda_P)]. \quad (\text{A17})$$

$\chi_{\bar{S}}$  and  $\chi_S$  are Gaussian and, respectively, given by

$$\begin{aligned} \chi_{\bar{S}}(\Lambda_P) &= \frac{1}{\pi^N} \int_{\mathbb{R}^{2N}} \chi_\rho(\Lambda_P, \Lambda_S) E(\Lambda_{\bar{S}}) \pi \delta^{(2)}(\Lambda_{s_N}) d^{2N} \Lambda_S \\ &= 2^{N-1} \|\gamma_{\bar{S}}\|^{-1/2} E[V_{\bar{S}}, 0](\Lambda_P), \end{aligned} \quad (\text{A18})$$

$$\begin{aligned} \chi_S(\Lambda_P) &= \frac{1}{\pi^N} \int_{\mathbb{R}^{2N}} \chi_\rho(\Lambda_P, \Lambda_S) E(\Lambda_S) d^{2N} \Lambda_S \\ &= 2^N \|\gamma_S\|^{-1/2} E[V_S, 0](\Lambda_P). \end{aligned} \quad (\text{A19})$$

Here the brackets  $\|\cdot\|$  refer to the determinant and

$$\begin{aligned} E[V, \bar{x}](B) &= \exp[-\frac{1}{2} B^T \Omega V \Omega^T B - i(\Omega \bar{x})^T B], \\ \gamma_{\bar{S}} &= \sigma_{\bar{S}} + I, \quad \gamma_S = \sigma_S + I, \\ V_{\bar{S}} &= \sigma_P - K_{\bar{S}} \gamma_{\bar{S}}^{-1} K_{\bar{S}}^T, \\ V_S &= \sigma_P - K_S \gamma_S^{-1} K_S^T. \end{aligned} \quad (\text{A20})$$

The normalization  $P(C)$  can be obtained by demanding that  $\chi_{\rho_c}(\Lambda_P = 0) = 1$ .  $E[V, \bar{x}](B)$  is the characteristic function of a Gaussian state with covariance matrix  $V$  and centered on position  $\bar{x}$  in phase space.

We now derive a closed-form expression for the correlator  $\langle \prod_{p \in P} M_p^{(n_p)} \rangle$ , describing correlations between the measurement outcomes obtained by the  $N$  parties. The characteristic function of the observable  $\prod_{p \in P} M_p^{(n_p)}$  is given by

$$\begin{aligned} \chi_M(\Lambda, X_P) &= \prod_{p \in P} \{ \pi \delta^{(2)}(\Lambda_p) - 2(1-p_d) E[I, -2X_p^{(n_p)}](\Lambda_p) \}. \end{aligned} \quad (\text{A21})$$

As we will show in the next section, when amplitude or phase noise is present, then we should instead use the characteristic function

$$\begin{aligned} \chi_M(\Lambda_P, X_P) &= \prod_{p \in P} \{ \pi \delta^{(2)}(\Lambda_p) - 2(1-p_d) E[\Delta_p^{(n_p)}, -2X_p^{(n_p)}](\Lambda_p) \}, \end{aligned} \quad (\text{A22})$$

where  $\Delta_p^{(n_p)}$  is the covariance matrix describing a noisy displacement for party  $p$ . We form the covariance matrix  $\Delta_P$ , describing the statistics of the noisy displacements for all  $N$  modes. We assume no correlation between noise in different modes, and  $\Delta_P$  is therefore block diagonal. The above product is rewritten as a sum over products,

$$\chi_M(\Lambda_P, X_P) = \sum_d [-2(1-p_d)]^{|d|} \prod_{p \in P} K_p^{(d_p)}, \quad (\text{A23})$$

where the sum runs over all binary lists  $d = (d_{p_1}, d_{p_2}, \dots, d_{p_N})$ .  $|d|$  is the sum of  $d$ , i.e., the number of ones in the list.  $K_p^{(d_p)}$  is the piecewise characteristic

function defined as

$$K_p^{(d_p)} = \begin{cases} \pi \delta^2(\Lambda_p) & \text{if } d_p = 0 \\ E[\Delta_p^{(n_p)}, -2X_p^{(n_p)}](\Lambda_p) & \text{if } d_p = 1 \end{cases}. \quad (\text{A24})$$

Given a Gaussian state  $\rho_G$  with characteristic function  $E[\sigma_G, 0](\Lambda_P)$ , we evaluate the expectation value of the observable,

$$\begin{aligned} f(\sigma_G, X_P) &= \text{Tr} \left\{ \rho_G \prod_{p \in P} M_p^{(n_p)} \right\} \\ &= \frac{1}{\pi^N} \int_{\mathbb{R}^{2N}} E[\sigma_G, 0](-\Lambda_P) \chi_M(\Lambda_P, X_P) d^{2N} \Lambda_P \\ &= \sum_d [-8\pi(1-p_d)]^{|d|} G[\sigma_G^{(d)} + \Delta_P^{(d)}, 0](2X_P^{(d)}). \end{aligned} \quad (\text{A25})$$

$\sigma_G^{(d)}$  is the submatrix of  $\sigma_G$  containing all the modes where  $d$  is 1; i.e., if  $d = (1, 0, 1, 1)$ , then we extract the covariance matrix describing the marginal distribution of modes  $p_1$ ,  $p_3$ , and  $p_4$ . Likewise, we have for the present example  $\Delta_P^{(d)} = \text{Diag}(\Delta_{p_1}^{(n_{p_1})}, \Delta_{p_3}^{(n_{p_3})}, \Delta_{p_4}^{(n_{p_4})})$  and  $X_P^{(d)} = X_{p_1}^{(n_{p_1})} \oplus X_{p_3}^{(n_{p_3})} \oplus X_{p_4}^{(n_{p_4})}$ . We have also defined the normal distribution,  $G[V, \bar{x}](X) = [(2\pi)^D \|V\|]^{-1/2} e^{-\frac{1}{2}(X-\bar{x})^T V^{-1}(X-\bar{x})}$ , where  $D$  is the dimension of  $V$ . Applying this result to the conditional state, which is a sum of two Gaussians, we obtain

$$\begin{aligned} \left\langle \prod_{p \in P} M_p^{(n_p)} \right\rangle &= \text{Tr} \left\{ \rho_c \prod_{p \in P} M_p^{(n_p)} \right\} \\ &= \frac{(1-p_d)^{N-1}}{P(C)} [2^{N-1} \|\gamma_S\|^{-\frac{1}{2}} f(V_S, X_P) \\ &\quad - 2^N (1-p_d) \|\gamma_S\|^{-\frac{1}{2}} f(V_S, X_P)]. \end{aligned} \quad (\text{A26})$$

This is a closed-form expression for the correlator of the measurements.

### a. Loss

A Gaussian transformation transforms the quadrature operators as  $Q \rightarrow SQ + d$ , where  $S$  is a symplectic matrix, i.e.,  $S\Omega S^T = \Omega$ , and  $d$  is a displacement [37,38]. Correspondingly, one can show that under a Gaussian transformation, the characteristic function transforms as

$$\chi(\Lambda) \rightarrow \exp(id^T \Omega \Lambda) \chi(S^{-1} \Lambda). \quad (\text{A27})$$

We note that  $S^{-1} = \Omega^T S^T \Omega$ . We model loss, acting on the optical modes of the system, by mixing said modes with a set of empty (ground-state) environmental modes, and subsequently trace out the environmental modes. Let the modes be ordered as  $\Lambda = \Lambda_P \oplus \Lambda_S \oplus \Lambda_E$ , where  $\Lambda_E$  are the conjugate quadratures for the environmental modes. We assume there is one environmental mode for each system mode ( $S, P$ ). The system modes and environmental modes are mixed using beamsplitter interactions, described by the symplectic matrix  $U_\eta$ ,

$$U_\eta = \begin{pmatrix} G_\eta^{1/2} & -\sqrt{I-G_\eta} \\ \sqrt{I-G_\eta} & G_\eta^{1/2} \end{pmatrix}. \quad (\text{A28})$$

By using Eq. (A13), Eq. (A27), and  $U_\eta$ , we obtain the map corresponding to loss acting on the system modes. This map transforms the characteristic function as

$$\chi(\Lambda) \rightarrow \chi(G_\eta^{1/2} \Lambda) \exp\left[-\frac{1}{2} \Lambda^T (I - G_\eta) \Lambda\right]. \quad (\text{A29})$$

Equation (17) can be derived from this mapping, and it can also be used to show that detector loss can be commuted through the interferometer B, given that all detectors have the same efficiency.

### b. Phase and amplitude noise

We now evaluate the effect of phase and amplitude noise on the computed correlators. Given that the optical state  $\rho$  is perturbed in phase by the environment, we model this by stochastic rotations in phase space  $\rho = \int d^N \theta P(\theta) R(\theta) \rho_0 R(-\theta)$ , where  $\rho_0$  is the unperturbed state,  $\theta = (\theta_{p_1}, \theta_{p_2}, \dots, \theta_{p_N})$  is a vector of stochastic rotation angles, and  $R(\theta)$  is the rotation operator  $R(\theta) = \prod_{p \in P} R_p(\theta_p)$ . We shift this stochastic rotation from the state onto the observable:

$$\begin{aligned} \left\langle \prod_{p \in P} M_p^{(n_p)} \right\rangle &= \text{Tr} \left\{ \prod_{p \in P} M_p^{(n_p)} \rho \right\} = \text{Tr} \left\{ \prod_{p \in P} M_p^{(n_p)} \int d^N \theta P(\theta) R(\theta) \rho_0 R(-\theta) \right\} = \text{Tr} \left\{ \int d^N \theta P(\theta) R(-\theta) \prod_{p \in P} M_p^{(n_p)} R(\theta) \rho_0 \right\} \\ &= \text{Tr} \left\{ \prod_{p \in P} \int d\theta_p P(\theta_p) R_p(-\theta_p) M_p^{(n_p)} R_p(\theta_p) \rho_0 \right\} = \text{Tr} \left\{ \prod_{p \in P} \tilde{M}_p^{(n_p)} \rho_0 \right\}, \end{aligned} \quad (\text{A30})$$

where  $\tilde{M}_p^{(n_p)}$  is the noisy observable. By factorizing the probability as  $P(\theta) = \prod_{p \in P} P(\theta_p)$ , we have tacitly assumed that there is no correlation in the phase noise acting on different modes. Inserting the expression for the observable  $M_p^{(n_p)}$ , we have

$$R_p(-\theta_p) M_p^{(n_p)} R_p(\theta_p) = I_p - 2(1-p_d) R_p(-\theta_p) | -X_p^{(n_p)} \rangle_p \langle -X_p^{(n_p)} | R_p(\theta_p). \quad (\text{A31})$$

For a coherent state  $| -X_p^{(n_p)} \rangle$ , we have that a small rotation is identical to a displacement acting orthogonal to the amplitude vector  $-X_p^{(n_p)}$ . An orthogonal vector can be constructed by acting with the symplectic form:  $-\omega(-X_p^{(n_p)})$ . With this in mind, we

make the substitution

$$R_p(\theta_p) \rightarrow D_p(\theta_p \omega X_p^{(n_p)}). \quad (\text{A32})$$

Imprecision in the measurement process, such as a noisy displacement, might lead to noise in the amplitude. We include this by also applying a stochastic displacement along the amplitude vector  $X_p^{(n_p)}$ . This stochastic displacement is given as a fraction  $\epsilon_p$  of the amplitude vector  $X_p^{(n_p)}$ , i.e., the stochastic displacement is  $\epsilon_p X_p^{(n_p)}$ .  $\epsilon_p$  is referred to as the relative amplitude. The noisy observable for party  $p$  is then given as

$$\begin{aligned} \tilde{M}_p^{(n_p)} &= \int d\theta_p d\epsilon_p P(\theta_p, \epsilon_p) D_p(-\theta_p \omega X_p^{(n_p)}) D_p(-\epsilon_p X_p^{(n_p)}) M_p^{(n_p)} D_p(\epsilon_p X_p^{(n_p)}) D_p(\theta_p \omega X_p^{(n_p)}) \\ &= I - 2(1 - p_d) \int P(\theta_p, \epsilon_p) |-(1 + \epsilon_p + \theta_p \omega) X_p^{(n_p)}\rangle \langle -(1 + \epsilon_p + \theta_p \omega) X_p^{(n_p)}| d\theta_p d\epsilon_p = I - 2(1 - p_d) \beta_p^{(n_p)}. \end{aligned} \quad (\text{A33})$$

$P(\theta_p, \epsilon_p)$  is the distribution over displacements, and we have introduced the state

$$\beta_p^{(n_p)} = \int P(\theta_p, \epsilon_p) |-(1 + \epsilon_p + \theta_p \omega) X_p^{(n_p)}\rangle \langle -(1 + \epsilon_p + \theta_p \omega) X_p^{(n_p)}| d\theta_p d\epsilon_p. \quad (\text{A34})$$

We model  $P(\theta_p, \epsilon_p)$  as a Gaussian, given by

$$P(\theta_p, \epsilon_p) = [(2\pi)^2 \|\Sigma_p\|]^{-1/2} \exp\left[-\frac{1}{2} \begin{pmatrix} \epsilon_p & \theta_p \end{pmatrix} \Sigma_p^{-1} \begin{pmatrix} \epsilon_p \\ \theta_p \end{pmatrix}\right]. \quad (\text{A35})$$

The covariance matrix is chosen to be diagonal,

$$\Sigma_p = \begin{pmatrix} V_A & 0 \\ 0 & V_\theta \end{pmatrix}. \quad (\text{A36})$$

$V_A$  and  $V_\theta$  are the relative amplitude and phase angle variances, respectively.  $\beta_p^{(n_p)}$  has a characteristic function given by

$$\begin{aligned} \chi_{\beta_p^{(n_p)}} &= \text{Tr} \{ \beta_p^{(n_p)} D_p(\Lambda_p) \} = \int P(\theta_p, \epsilon_p) E[I, -(1 + \epsilon_p + \theta_p \omega) 2X_p^{(n_p)}](\Lambda_p) d\theta_p d\epsilon_p \\ &= E[I + V_A (2X_p^{(n_p)}) \otimes (2X_p^{(n_p)})^T + V_\theta (\omega^T 2X_p^{(n_p)}) \otimes (\omega^T 2X_p^{(n_p)})^T, -2X_p^{(n_p)}](\Lambda_p). \end{aligned} \quad (\text{A37})$$

So the effect of amplitude and phase noise is to broaden the phase space distribution of  $\beta_p^{(n_p)}$  along  $2X_p^{(n_p)}$  and  $\omega^T 2X_p^{(n_p)}$ . We define the covariance matrix of the state  $\beta_p^{(n_p)}$  as  $\Delta_p^{(n_p)}$ ,

$$\Delta_p^{(n_p)} = I + V_A (2X_p^{(n_p)}) \otimes (2X_p^{(n_p)})^T + V_\theta (\omega^T 2X_p^{(n_p)}) \otimes (\omega^T 2X_p^{(n_p)})^T. \quad (\text{A38})$$

## 2. A2

Let  $n$  be a binary list of measurement settings, and  $g$  a binary list of measurement outcomes for the detectors in  $P$ , where click corresponds to 1 and no click corresponds to 0. We may then compute the probability of obtaining the outcomes  $g$  using the characteristic function  $\chi_{\rho_c}$ . This probability is given by the expression

$$\begin{aligned} P_Q(g|n) &= \frac{(1 - p_d)^{N-1}}{P(C)} \left[ 2^{N-1} \|\gamma_S\|^{-\frac{1}{2}} h_g(V_S) \right. \\ &\quad \left. - 2^N (1 - p_d) \|\gamma_S\|^{-\frac{1}{2}} h_g(V_S) \right], \end{aligned} \quad (\text{A39})$$

where

$$\begin{aligned} h_g(V) &= [4\pi(1 - p_d)]^{|\bar{g}|} \sum_b [-4\pi(1 - p_d)]^{|b|} G[V^{(b+\bar{g})} \\ &\quad + \Delta_p^{(b+\bar{g})}, 2X_p^{(b+\bar{g})}]. \end{aligned} \quad (\text{A40})$$

$\bar{g}$  is the negation of  $g$ , i.e., we replace 1 by 0 and vice versa. The measurement settings  $n$  define the arrays  $\Delta_p$

and  $X_p$ . The sum runs over all binary lists  $b$  of length  $N$ , satisfying the constraint that  $b$  takes the value zero in positions where  $g$  takes the value zero. For example, if  $g = (1, 0, 0, 1)$ , then the sum would run over the lists  $b \in \{(0, 0, 0, 0), (1, 0, 0, 0), (0, 0, 0, 1), (1, 0, 0, 1)\}$ .  $V^{(b+\bar{g})}$  is the submatrix of the covariance matrix  $V$ , containing all the modes where the vector  $b + \bar{g}$  takes the value 1; e.g., if  $b + \bar{g} = (0, 1, 1, 1)$  then the marginal covariance matrix describing modes  $p_2, p_3$ , and  $p_4$  is extracted. Marginal probabilities for a subset of parties A can be extracted from  $P_Q(g|n)$  by summing over outcomes for the remaining parties B. The measurement settings for subset B should be fixed during this summation; however, the choice of settings for B is arbitrary owing to the no-signalling property of quantum mechanics [13].

We then want to determine whether the array  $P_Q(g|n)$  can be expressed as a convex sum of local response functions. Let  $L(g_p|n_p, \lambda_k)$  be the local response function for party  $p$ , determined by the hidden variables  $\lambda_k$ . The response function gives the probability of party  $p$  obtaining a particular outcome  $g_p$ , given the measurement setting  $n_p$  and hidden variables  $\lambda_k$ .

We determine whether there exists a set of coefficients  $c_k$  such that [13]

$$P_Q(g|n) = \sum_k c_k \prod_{p \in P} L(g_p | n_p, \lambda_k), \quad \sum_k c_k = 1, \quad c_k \geq 0. \quad (\text{A41})$$

$c_k$  is interpreted as the probability that the hidden variables  $\lambda_k$  are shared by the parties in a given measurement round. We use the set of deterministic response functions, i.e., each response function can be written as a Kronecker delta function,

$$L(g_p | n_p, \lambda_k) = \delta(g_p, g_{n_p, \lambda_k}). \quad (\text{A42})$$

$g_p$  is a potential outcome for party  $p$ , and  $g_{n_p, \lambda_k}$  is the outcome that is actually obtained, given the hidden variables  $\lambda_k$  and the setting  $n_p$ . Whether the set of requirements in Eq. (A41) allows for a solution or not, is determined using the `linprog` module of the SciPy 1.8.1 package in Python. When no solution is present, we know that the array of probabilities  $P_Q(g|n)$ , determined by the quantum state, does not admit a local hidden variable model. In this case  $P_Q(g|n)$  lies outside the Bell polytope. However, when a solution is present we know that the system can be described by a local hidden variable model, and no Bell inequality can be violated.

- 
- [1] I. Pitowsky, George Boole's 'conditions of possible experience' and the quantum puzzle, *Brit. J. Philos. Sci.* **45**, 95 (1994).
- [2] J.-D. Bancal, N. Gisin, and S. Pironio, Looking for symmetric Bell inequalities, *J. Phys. A: Math. Theor.* **43**, 385303 (2010).
- [3] J. Bell, On the Einstein Podolsky Rosen paradox, *Phys. Phys. Fiz.* **1**, 195 (1964).
- [4] J. S. Bell, *Speakable and Unsayable in Quantum Mechanics* (Cambridge University Press, Cambridge, 2013).
- [5] A. Aspect, J. Dalibard, and G. Roger, Experimental Test of Bell's Inequalities Using Time-Varying Analyzers, *Phys. Rev. Lett.* **49**, 1804 (1982).
- [6] A. Aspect, P. Grangier, and G. Roger, Experimental Realization of Einstein-Podolsky-Rosen-Bohm *Gedankenexperiment*: A New Violation of Bell's Inequalities, *Phys. Rev. Lett.* **49**, 91 (1982).
- [7] S. J. Freedman and J. F. Clauser, Experimental Test of Local Hidden-Variable Theories, *Phys. Rev. Lett.* **28**, 938 (1972).
- [8] B. Hensen, H. Bernien, A. E. Dr  au, A. Reiserer, N. Kalb, M. S. Blok, J. Ruitenberg, R. F. L. Vermeulen, R. N. Schouten, C. Abell  n *et al.*, Loophole-free Bell inequality violation using electron spins separated by 1.3 kilometres, *Nature (London)* **526**, 682 (2015).
- [9] L. K. Shalm, E. Meyer-Scott, B. G. Christensen, P. Bierhorst, M. A. Wayne, M. J. Stevens, T. Gerrits, S. Glancy, D. R. Hamel, M. S. Allman *et al.*, Strong Loophole-Free Test of Local Realism, *Phys. Rev. Lett.* **115**, 250402 (2015).
- [10] M. Giustina, M. A. M. Versteegh, S. Wengerowsky, J. Handsteiner, A. Hochrainer, K. Phelan, F. Steinlechner, J. Kofler, J. A. Larsson, C. Abellan *et al.*, Significant-Loophole-Free Test of Bell's Theorem with Entangled Photons, *Phys. Rev. Lett.* **115**, 250401 (2015).
- [11] W. Rosenfeld, D. Burchardt, R. Garthoff, K. Redeker, N. Ortegel, M. Rau, and H. Weinfurter, Event-Ready Bell Test Using Entangled Atoms Simultaneously Closing Detection and Locality Loopholes, *Phys. Rev. Lett.* **119**, 010402 (2017).
- [12] J. Wilms, Y. Disser, G. Alber, and I. C. Percival, Local realism, detection efficiencies, and probability polytopes, *Phys. Rev. A* **78**, 032116 (2008).
- [13] N. Brunner, D. Cavalcanti, S. Pironio, V. Scarani, and S. Wehner, Bell nonlocality, *Rev. Mod. Phys.* **86**, 419 (2014).
- [14] I. Gerhardt, Q. Liu, A. Lamas-Linares, J. Skaar, V. Scarani, V. Makarov, and C. Kurtsiefer, Experimentally Faking the Violation of Bell's Inequalities, *Phys. Rev. Lett.* **107**, 170404 (2011).
- [15] W. Zhang, T. van Leent, K. Redeker, R. Garthoff, R. Schwonek, F. Fertig, S. Eppelt, W. Rosenfeld, V. Scarani, C. C.-W. Lim, and H. Weinfurter, A device-independent quantum key distribution system for distant users, *Nature (London)* **607**, 687 (2022).
- [16] S. Pironio, A. Ac  n, N. Brunner, N. Gisin, S. Massar, and V. Scarani, Device-independent quantum key distribution secure against collective attacks, *New J. Phys.* **11**, 045021 (2009).
- [17] A. Ac  n, N. Gisin, and L. Masanes, From Bell's Theorem to Secure Quantum Key Distribution, *Phys. Rev. Lett.* **97**, 120405 (2006).
- [18] R. Arnon-Friedman, F. Dupuis, O. Fawzi, R. Renner, and T. Vidick, Practical device-independent quantum cryptography via entropy accumulation, *Nat. Commun.* **9**, 459 (2018).
- [19] A. K. Ekert, Quantum Cryptography Based on Bell's Theorem, *Phys. Rev. Lett.* **67**, 661 (1991).
- [20] U. Vazirani and T. Vidick, Fully Device-Independent Quantum Key Distribution, *Phys. Rev. Lett.* **113**, 140501 (2014).
- [21] J. B. Brask and R. Chaves, Robust nonlocality tests with displacement-based measurements, *Phys. Rev. A* **86**, 010103(R) (2012).
- [22] M. Żukowski, A. Zeilinger, M. A. Horne, and A. K. Ekert, "Event-ready-detectors" Bell experiment via entanglement swapping, *Phys. Rev. Lett.* **71**, 4287 (1993).
- [23] L.-M. Duan, M. D. Lukin, J. I. Cirac, and P. Zoller, Long-distance quantum communication with atomic ensembles and linear optics, *Nature (London)* **414**, 413 (2001).
- [24] U. L. Andersen and T. C. Ralph, High-Fidelity Teleportation of Continuous-Variable Quantum States Using Delocalized Single Photons, *Phys. Rev. Lett.* **111**, 050504 (2013).
- [25] C. H. Bennett, G. Brassard, C. Crepeau, R. Jozsa, A. Peres, and W. K. Wootters, Teleporting an Unknown Quantum State via Dual Classical and Einstein-Podolsky-Rosen Channels, *Phys. Rev. Lett.* **70**, 1895 (1993).
- [26] S. L. Braunstein and A. Mann, Measurement of the Bell operator and quantum teleportation, *Phys. Rev. A* **51**, R1727 (1995).
- [27] J. B. Brask, R. Chaves, and N. Brunner, Testing nonlocality of a single photon without a shared reference frame, *Phys. Rev. A* **88**, 012111 (2013).
- [28] A. Laghaout, G. Bj  rk, and U. L. Andersen, Realistic limits on the nonlocality of an N-partite single-photon superposition, *Phys. Rev. A* **84**, 062127 (2011).
- [29] R. Chaves and J. B. Brask, Feasibility of loophole-free nonlocality tests with a single photon, *Phys. Rev. A* **84**, 062110 (2011).
- [30] T. Ralph and A. Lund, Nondeterministic noiseless linear amplification of quantum systems, *AIP Conf. Proc.* **1110**, 155 (2009).



- [31] R. F. Werner and M. M. Wolf, All-multipartite Bell-correlation inequalities for two dichotomic observables per site, *Phys. Rev. A* **64**, 032112 (2001).
- [32] H. Weinfurter and M. Żukowski, Four-photon entanglement from down-conversion, *Phys. Rev. A* **64**, 010102(R) (2001).
- [33] M. Żukowski and Časlav Brukner, Bell's Theorem for General  $N$ -Qubit States, *Phys. Rev. Lett.* **88**, 210401 (2002).
- [34] R. F. Werner and M. M. Wolf, Bell inequalities and entanglement, *Quantum Inf. Comput.* **1**, 1 (2001), [arXiv:quant-ph/0107093](https://arxiv.org/abs/quant-ph/0107093).
- [35] G. Bacciagaluppi and R. Hermens, Bell-inequality violation and relativity of pre- and postselection, *Phys. Rev. A* **104**, 012201 (2021).
- [36] G. S. Agarwal, *Quantum Optics* (Cambridge University Press, Cambridge, 2013).
- [37] C. Weedbrook, S. Pirandola, R. García-Patrón, N. J. Cerf, T. C. Ralph, J. H. Shapiro, and S. Lloyd, Gaussian quantum information, *Rev. Mod. Phys.* **84**, 621 (2012).
- [38] A. Ferraro, S. Olivares, and M. G. A. Paris, Gaussian states in continuous variable quantum information, [arXiv:quant-ph/0503237](https://arxiv.org/abs/quant-ph/0503237).